Histidine is a source of the anti-oxidant, α-ketoglutarate in *Pseudomonas fluorescens* challenged by oxidative stress

Joseph Lemire ,Yves Milandu , Christopher Auger, Adam Bignucolo, Varun P. Appanna and Vasu D. Appanna*

Department of Chemistry and Biochemistry

Laurentian University

Sudbury, Ontario

Canada P3E 2C6

*corresponding author

Phone: (705) 675-1151 ext. 2112
Fax: (705) 675-4844
Email: vappanna@laurentian.ca

This is an Accepted Article that has been peer-reviewed and approved for publication in the *FEMS Microbiology Letters*, but has yet to undergo copy-editing and proof correction. Please cite this article as an "Accepted Article"; doi: 10.1111/j.1574-6968.2010.02034.x

Abstract:

The role of α-ketoglutarate (KG) in the detoxification of reactive oxygen species (ROS) has only recently begun to be appreciated. This keto acid neutralizes ROS in an NADPH-independent manner with the concomitant formation of succinate and CO_2. To further probe this intriguing attribute of KG in living systems, we have evaluated the significance of histidine metabolism in the model organism, *Pseudomonas fluorescens* challenged by hydrogen peroxide (H_2O_2). Here we show that this amino acid does contribute to KG homeostasis and appears to be earmarked for the production of KG during oxidative stress. Both the NAD and NADP dependent glutamate dehydrogenases (GDH) were upregulated in the stressed cells despite the sharp decline in the activities of numerous enzymes mediating the tricarboxylic acid (TCA) cycle and the oxidative phosphorylation. Enzymes such as isocitrate dehydrogenase (ICDH)-NAD dependent, succinate dehydrogenase (SDH), α-ketoglutarate dehydrogenase (KGDH), Complex I and Complex IV were severely affected in the *P. fluorescens* grown in the presence of H_2O_2. Studies with fluorocitrate, a potent inhibitor of citrate metabolism clearly revealed that histidine was preferentially utilized in the production of KG in the H_2O_2–challenged cells. Regulation experiments also helped confirm that the metabolic reprogramming resulting in the enhanced production of KG was evoked by H_2O_2 stress. These data further establish the pivotal role KG plays in anti-oxidative defense.

Keywords: oxidative stress – α-ketoglutarate – histidine – *Pseudomonas fluorescens* – glutamate dehydrogenase – metabolic reprogramming

Introduction:

Oxidative stress is a constant hazard of aerobic life. All organisms that utilize O_2 to maximize ATP production during oxidative phosphorylation are exposed to the dangers associated with the ROS, namely superoxide ($O_2^{\bullet -}$), peroxide (H_2O_2), and $OH^{\bullet}$ (James, *et al.*, 2005). These oxidative moieties are primarily generated as a consequence of electron transport to O_2 (DeJong, *et al.*, 2007). Hence, it is pivotal that aerobic organisms nullify these toxicants if they are to survive an O_2-rich environment. Indeed, aerobic living systems have evolved numerous intricate stratagems in response to the ongoing menace posed by oxidative stress (Cabiscol, *et al.*, 2000, Imlay, 2008, Maaty, *et al.*, 2009). Superoxide dismutase (SOD), glutathione peroxidase and thioredoxin peroxidases are some of the enzymes that are involved in the direct elimination of $O^{\bullet -}_2$ and H_2O_2 (DeJong, *et al.*, 2007). Indeed, *P.fluorescens* is known to utilize these ROS-scavengers (Singh, 2005, Singh, *et al.*, 2007).

However, these enzymatic processes tend to be ineffective if the reductive potential of the cell is not replenished (Dringen, 2005, Cappellini & Fiorelli, 2008). NADPH is the key molecule that powers these anti-oxidative defense mechanisms and helps maintain the proper redox balance. During oxidative stress, NADPH-generating systems such as glucose 6 phosphate dehydrogenase (G6PDH), malic enzyme (ME) and isocitrate dehydrogenase (ICDH)-NADP are upregulated (Beriault, *et al.*, 2005, Singh, *et al.*, 2007). Indeed, when *P. fluorescens* is exposed to H_2O_2, the overexpression of G6PDH and its isozymes has been observed. The enhanced activities of ICDH-NADP and malic enzyme (ME) have also been demonstrated in various organisms (Dringen, 2005, Smeets, *et al.*, 2005, Valderrama, *et al.*, 2006). In fact, the former enzyme has

been shown to be a key provider of NADPH in the peroxisome, an organelle which is subjected to heightened levels of H_2O_2 (Henke, *et al.*, 1998). The involvement of metabolic networks designed to supplement the need of NADPH has also been recently uncovered. These metabolic modules not only lead to the increased production of NADPH but also impede the formation of NADH, a pro-oxidant moiety known to augment the oxidative burden of the cell (Finkel & Holbrook, 2000, Singh, *et al.*, 2008).

The role of nicotinamide adenine dinucleotide kinase (NADK) in promoting the production of NADP, a critical cofactor for NADPH-generating enzymes and in alleviating oxidative stress has only recently begun to emerge (Singh, *et al.*, 2007). We have also shown that the TCA cycle is reconfigured to limit the production of NADH and increase the formation of the keto acid, α-ketoglutarate. This is achieved by the decrease in the expression of KGDH, and the downregulation of ICDH-NAD and the increase in ICDH-NADP. These enzymes partner together to create a pool of KG that detoxifies ROS. This NADPH-independent anti-oxidative defense mechanism leads to the production of succinate, a signaling molecule that helps promote anaerobiosis in numerous systems (Mailloux, *et al.*, 2007, Mailloux, *et al.*, 2009).

As part of our study to delineate the link between metabolism, aerobiosis and anti-oxidative defense, we have examined the influence of histidine on the KG homeostasis during oxidative stress in *P. fluorescens*, a microbe known for its nutritional versatility and metabolic adaptability. Here, we demonstrate that this amino acid is indeed a source of KG when this microbe is confronted with H_2O_2 insult. Its degradation via glutamate provides an easy access to this keto acid. The production of KG appears to be mediated

by the enhanced activity of GDH and diminished expression of KGDH. The significance of KG as an anti-oxidant is also discussed.

Material and Methods

Conditions for microbial growth

P. fluorescens (ATCC 13525), was obtained from the American Type Culture Collection. It was maintained and grown in a minimal mineral medium consisting of Na_2HPO_4 (6.0g), KH_2PO_4 (3.0g), $MgSO_4.7H_2O$ (0.2g), 15mM histidine (2.3g), and 19mM citrate (2.7g) per litre of deionized water. Trace elements were added in concentrations as previously described in (Mailloux, *et al.*, 2009). Oxidative stress was induced by adding either 100 μM or 500 μM of H_2O_2 these concentrations of H_2O_2 were added to the medium prior to the bacterial inoculation. To ensure that the H_2O_2 levels remained relatively constant, a second dose of the oxidant was introduced after 20-24h of microbial growth (Most experiments were performed in cells exposed to 500μM H_2O_2 as this concentration of the oxidant did not significantly affect cellular yield and elicited marked metabolic responses). The pH was adjusted to 6.8 with dilute NaOH. The media was then dispensed into 200 ml amounts in 500 ml Erlenmeyer flasks, stoppered with foam plugs, and autoclaved for 20 min at 121 ^{o}C. Inoculations were made with 1ml of stationary-phase cells grown in a stressed-free medium in an aerated gyratory water bath shaker, model 76 (New Brunswick Scientific) at 26 ^{o}C at 140 rpm. Cells and spent fluids were isolated at various growth phases. These were subsequently utilized for enzymatic, HPLC, western blot, and biomass studies (24h for control and 28h for H_2O_2-stressed cultures corresponded to similar growth phase). For growth measurements, 10 mL of

bacterial cultures were utilized and solubilized protein contents were monitored by the Bradford method using the Bio-Rad Protein Assay reagent (Bradford, 1976).

Cellular fractionation

P. fluorescens cells were isolated at similar growth phases and resuspended in a cell storage buffer (CSB) consisting of 50 mM Tris-HCl, 5 mM $MgCl_2$, 1mM phenylmethylsulphonyl fluoride (PMSF) (pH 7.3). The cells were lysed by sonication and then centrifuged at 3,000 x g for 30 min at 4 ^{o}C to remove intact bacteria. Centrifugation at 180,000 x g for 3h yielded a soluble cell free extract (CFE) and a membrane CFE. The soluble fraction was further centrifuged at 180,000 x g for 1h to obtain a membrane-free system. The purity of these fractions were determined by monitoring glucose-6-phosphate dehydrogenase activity for the soluble component and Complex I activity for the membrane fraction. The protein content in the soluble and membrane fractions was determined using the Bradford assay (Bradford, 1976). These CFE fractions were kept at 4^{o}C for up to 5 days and various enzymatic activities were monitored.

Metabolite Analyses

Various metabolite levels were determined by HPLC. Cells and spent fluids from the control and H_2O_2 stressed cultures were harvested at similar growth phases. Whole cells were homogenized by sonication as described above to yield CFE and then subjected to HPLC analysis following the treatment of the CFE (2mg protein equivalent) with 0.5% v/v of perchloric acid for 10min on ice. The precipitate was removed by

centrifugation. The supernatant was then filtered and injected into an Alliance HPLC equipped with a C_{18} reverse-phase column (Synergi Hydro-RP; 4µm; 250 x 4.6mm, Phenomenex) operating at a flow rate of 0.7mL/min at ambient temperature. This flow rate was utilized for the identification of organic acids, which were monitored at 210nm. A mobile phase consisting of 20mM K_2HPO_4 (pH 2.9) was used to separate the organic acids. All the metabolites in this study were identified using known standards and the peaks were quantified using the Empower Software (Waters Corporation). The HPLC was standardized using a five-point calibration prior to each injection protocol. Peaks were routinely spiked with known standards to confirm their identities.

Blue Native PAGE and in-gel activity staining

Blue Native (BN) polyacrylamide gel electropohoresis (PAGE) was performed following a modified method described previously (Schagger & von Jagow, 1991, Mailloux, *et al.*, 2009). Cellular fractions isolated from *P. fluorescens* were prepared in a non-denaturing buffer (50mM Bis-Tris, 500mM ε-aminocaproic acid, pH 7.0, 4°C) at a final concentration of 4mg of protein per ml. For the membrane CFE, 1% (v/v) β-dodecyl-D-maltoside was added to the preparation to facilitate the solubilization of the membrane-bound proteins. To ensure optimal protein separation, 4-16% linear gradient gels were cast with the Bio-Rad MiniProtean^{TM} 2 system using 1mm spacers. Soluble or membrane proteins (60µg) were loaded into the wells and the gels were electrophoresed under native conditions. 80V was applied for the stacking gel. The voltage was then increased to 300V once the running front entered the separating gel. The blue cathode buffer (50mM Tricine, 15min Bis-Tris, 0.02% (w/v) Coomassie G-250 (pH 7) at 4°C) was changed to a colorless cathode buffer (50mM Tricine, 15min Bis-Tris, (pH 7) at 4°C)

when the running front was half-way through the gel. Upon completion, the gel slab was equilibrated for 15min in a reaction buffer. The in-gel visualization of enzyme activity was ascertained by coupling the formation of NAD(P)H to 0.3mg/mL of phenazine methosulfate (PMS) and 0.5mg/mL of iodonitrotetrazolium (INT). ICDH-NADP activity was visualized using a reaction mixture consisting of reaction buffer, 5mM isocitrate, 0.1 - 0.5mM NADP, INT, and PMS. The same reaction mixture was utilized for ICDH-NAD except for 0.1 – 0.5mM NAD. GDH-NAD activity was visualized using a reaction mixture consisting of reaction buffer, 5mM glutamate, 0.1 - 0.5mM NAD, INT, and PMS. GDH-NADP activity was visualized using a reaction mixture consisting of reaction buffer, 5mM glutamate, 0.5mM NADP, INT, and PMS. KGDH activity was visualized using a reaction mixture consisting of reaction buffer, 5mM KG, 0.5mM NAD, 0.1mM CoA, INT, and PMS. Glutamate synthase (GS) activity was determined employing a reaction mixture consisting of reaction buffer, 5mM glutamine, 0.5mM NADPH, 5mM KG, 5units/mL GDH, INT and 0.0167 mg/mL of 2,4-dichloroindophenol (DCIP). Complex 1 was detected by the addition of 1 mM NADH, and INT. 40 μM rotenone was added to inhibit the complex. SDH was monitored by the addition of 5 mM succinate, INT, and PMS. Complex IV was assayed by the addition of 10 mg/mL of diaminobenzidine, 10 mg/mL cytochrome C, and 562.5 mg/mL of sucrose. 5 mM KCN was added to the reaction mixture to confirm the identity of Complex IV. Aspartate amino transferase (AST) was monitored by the addition of 5 mM aspartate, 5 mM KG, 0.5 mM NADP, 5 units of GDH, INT, and PMS. The formation of glutamate effected by AST under these conditions was detected by GDH.

Reactions were halted using destaining solution (40% methanol, 10% glacial acetic acid) once the activity bands reached their desired intensities. Activity stains performed in the absence of substrate and/or in the presence of inhibitors assured band specificity. Coomassie staining for total proteins determined proper protein loading. Enzyme reactions were confirmed by monitoring the formation of products as well as the disappearance of reactants by incubating the activity bands with the appropriate reaction mixtures.

Western Blotting Technique for GDH Expression.

GDH expression was determined utilizing the method described in (Mailloux*, et al.*, 2009). Briefly, the protein samples were solubilized in 62.5 mM Tris-HCl (pH 6.8), 2% SDS, and 2% β-mercaptoethanol at 100°C for 5 min. Following solubilization, the protein samples were then loaded into a 10% isocratic gel and electrophoresed using a discontinuous buffer system. Following electrophoresis, the proteins were transferred electrophoretically to a Hybond™-Polyvinylidene difluoride membrane for immunoblotting. Non-specific binding sites were blocked by treating the membrane with 5% non-fat skim milk dissolved in TTBS [20 mM Tris-HCl, 0.8% NaCl, 1% Tween-20 (pH 7.6)] for 1 h. Polyclonal antibodies for GDH were obtained from Abcam. The secondary antibodies (Licor) consisted of infrared 700nm tagged goat anti-rabbit. Visualization of the immunoblot was documented via an Odysey infrared imaging system (Li-Cor, Lincoln Nebraska, USA).

Regulation experiments

The H_2O_2-mediated regulation of KGDH, GDH and ICDH was studied as follows. Ten milligrams of protein equivalent of H_2O_2-treated cells were transferred into the control (without H_2O_2) medium and a 10mg protein equivalent of control cells were incubated in a 100μM/ 500μM H_2O_2 containing media. Following a 4-8h incubation period, the cells were isolated and fractionated as described previously to determine enzymatic activities and/or expression. For proper comparison, control cells (24h) and H_2O_2-treated (28h) in similar growth phase were utilized to inoculate the different media, respectively.

Origin of KG in H_2O_2 stressed cells and histidine metabolism

Two milligrams of protein equivalent of CFE from control and stressed cells were placed in a reaction mixture consisting of 5mM histidine, 5mM citrate, in the presence or absence of 5mM fluorocitrate, an inhibitor of aconitase, in a phosphate buffer (Nasser, *et al.*, 2006). After 30min, the reaction was halted by placing the mixture at 100°C for 10min. The reaction mixture was then subjected to HPLC analysis to monitor the production of KG.

Statistical analysis

Data were expressed as means ± standard deviations. Statistical correlations of data were checked for significance using the Student t test ($p \leq 0.05$). All experiments were performed at least twice and in triplicate.

Results and Discussion:

Growth profile and metabolomic studies

While both citrate and histidine were readily utilized by the microbe, it appeared that at stationary phase of growth, nearly all the amino acid was consumed (Figure 1). The biomass yield was relatively similar in these two situations with the H_2O_2 – stressed bacteria attaining the stationary phase of growth at a slightly later time. Metabolomic analyses of the CFEs revealed that the H_2O_2-stressed cells contained significantly more KG and succinate (Figure 2). While intracellular levels of histidine were lower in the cells subjected to H_2O_2, citrate levels were relatively higher. These data pointed to the disparate metabolic networks operative in these systems and to the possible accumulation of KG and its utilization in combating oxidative stress. It has been shown that KG is involved in the detoxification of ROS with the concomitant formation of succinate. Ketoacids are known to eliminate ROS in a non-enzymatic manner (Brookes, *et al.*, 2006, Fedotcheva, *et al.*, 2006). Hence, it is not unlikely that *P.fluorescens* reprogrammed its metabolism in an effort to generate KG during the challenge posed by H_2O_2. This ketoacid has been shown to contribute to the dimunition of oxidative tension (Li, *et al.*, 2009). The increased presence of succinate and KG in stressed cells would point to such a possibility. As KG was an important metabolite during oxidative stress, its utilization and production were monitored.

KG homeostasis and NADPH production during oxidative stress

ICDH, KGDH, and GDH are the three main participants in modulating the concentration of KG. In this study there was a sharp increase in ICDH-NADP with the

concomitant decrease in KGDH in the cells challenged by H_2O_2. As histidine was the only source of nitrogen and a possible precursor of KG, the presence of GDH-NAD and GDH-NADP were probed. Although GDH-NADP was barely discernable in the control cells, there was a marked increase in the H_2O_2-stressed cells. While there was a mild increase in GDH-NAD, ICDH-NAD was sharply diminished in the H_2O_2-challenged cells. This is not surprising as NADH, a pro-oxidant is known to further exacerbate the oxidative burden of the cell (Finkel & Holbrook, 2000, Thomas, *et al.*, 2009). Hence, the H_2O_2-stressed *P. fluorescens* may have downregulated its formation. However, the upregulation of the NADPH production will be beneficial as this moiety plays a pivotal role in maintaining the reductive force of the microbe during oxidative stress. Furthermore, the enhancement of these enzymatic reactions (ICDH-NADP, and GDH-NADP) will lead to the production of KG (Mailloux, *et al.*, 2009). The diminution of KGDH has the net effect of increasing the pool of KG, a key contributor to the elimination of H_2O_2 (Brookes, *et al.*, 2006, Fedotcheva, *et al.*, 2006). Furthermore, the KGDH-mediated reaction has been shown to generate ROS (Starkov, *et al.*, 2004). To ascertain that the direct interaction between histidine and H_2O_2 does not lead to KG production, the growth medium with added H_2O_2 was monitored for 48h without *P.fluorescens.* No KG was discerned (data not included).

Hence, its down-regulation will quell the oxidative burden of the microbe, and limit the synthesis of NADH, a pro-oxidant. Thus, the enhanced activities of ICDH-NADP, and GDH-NADP coupled with the decreased activity of ICDH-NAD and KGDH help generate KG and NADPH, two key ingredients necessary for survival during oxidative stress. As glutamate was an important supplier of KG, it was important to

evaluate the status of other enzymes involved in the utilization or formation of this substrate. AST and GS are two potential candidates (Prell & Poole, 2006). There were no significant changes in these enzymes in the cells exposed to H_2O_2 (Figure 3). Hence, these data point to the channeling of substrates towards the formation of KG and NADPH with the subsequent decrease in the synthesis of NADH. This strategy ensures that during oxidative stress sufficient NADPH, a potent reductive fuel and KG a powerful scavenger of ROS, are available. The diminution in the generation of NADH will further help decrease the oxidative burden as this moiety drives the production of ROS via the electron transport chain.

Severely diminished electron transport chain during H_2O_2 *insult*

Furthermore, it is critical that during oxidative stress, the effectors mediating ROS production be attenuated. Oxidative phosphorylation is a major generator of ROS (Ludwig*, et al.*, 2001, Murphy, 2009). Hence, it is quite conceivable that the complexes mediating this process are downgraded. These Fe-containing complexes are susceptible to H_2O_2 (Touati, 2000, Middaugh*, et al.*, 2005). Indeed, there was a sharp reduction observed in the activities of Complex I, II, and IV (Figure 4). The nature of Complex I and IV were further confirmed by the inclusion of rotenone and KCN in the assay mixture. The former is a specific inhibitor for Complex I, while Complex IV is inhibited by KCN. The activity band was not detected in the control CFE in the presence of these inhibitors respectively (data not included). This strategy of limiting the formation of NADH coupled with diminished activities of the enzymes involved in its oxidation provides an effective tool to mitigate H_2O_2 insult. *P.fluorescens* appears to adopt this tactic in an effort to survive the oxidative environment promoted by H_2O_2. Numerous

organisms do indeed resort to diminished oxidative phosphorylation and anaerobiosis with the goal of fending a ROS challenge (Chen*, et al.*, 2003, Chenier*, et al.*, 2008). In eukaryotic systems, the promotion of the hypoxia inducible factor (HIF-1α), an activator of anaerobic respiration is favoured (Mailloux*, et al.*, 2009).

Modulation of KG by H_2O_2

As the catabolism of histidine was providing glutamate, a moiety involved in the generation of the anti-oxidant KG, it was important to ascertain if the enzymes involved in the formation and utilization of KG were modulated by H_2O_2. When control cells were exposed to H_2O_2 stress, the decrease in KGDH activity was coupled to the increase in GDH activity. However, when H_2O_2-stressed cells were introduced into control media, the reverse trend was observed i.e. the activity of KGDH was recovered while the activity of GDH was diminished. Western blot analyses revealed that the latter enzyme was more abundant in the H_2O_2-treated cells and was affected by this oxidative modulator (Figure 5). Hence, it is clear that H_2O_2 was indeed controlling the status of KGDH, GDH and ICDH and subsequently the levels of KG and NADPH. We have recently shown that the sulfhydryl group in the lipoic acid of KGDH may be a sensor of an oxidative environment (Mailloux*, et al.*, 2009). Its oxidation during menadione stress, a potent generator of $O^{\bullet}_2$ may help signal oxidative stress and the inactivation of KGDH. With the concomitant increased in GDH and ICDH activities observed in this study, it is quite plausible that the pool of KG created helps scavenge the ROS in a non-enzymatic manner. The presence of elevated amounts of succinate, a product of the decarboxylation of KG by ROS, in the H_2O_2 – stressed cells would point to such a possibility. Hence, *P.*

fluorescens appears to invoke the participation of KG in the detoxification of $O_2^{\bullet-}$ and H_2O_2.

Histidine the generator of KG

In order to decipher whether histidine metabolism was an important generator of KG during oxidative stress, the cellular extracts were treated with fluorocitrate. This moiety is known to interfere with citrate metabolism (Nasser*, et al.*, 2006, Zielke*, et al.*, 2007). Hence, the catabolism of citrate via aconitase should be perturbed and any KG formed would emanate from the degradation of histidine. In the H_2O_2 - stressed cultures, there was no sharp variation in the production of KG in the presence of fluorocitrate. However, in the control cultures, the inclusion of fluorocitrate led to only minute amounts of KG (Figure 6). As the citrate decomposition pathway was blocked in both cases, it is clear that the elevated levels of KG observed in the H_2O_2-stressed bacteria was due to the ability of H_2O_2 -challenged *P. fluorescens* to preferentially metabolize histidine to KG, an attribute absent in the control bacteria. Hence, it is within the realm of possibilities that *P. fluorescens* diverts histidine towards KG in an effort to combat oxidative stress. The role of keto-acids as anti-oxidants is now beginning to emerge. Both prokaryote and eukaryotes are known to invoke the enhanced production of these moieties to combat an oxidative environment (Brookes*, et al.*, 2006, Mailloux*, et al.*, 2007, Sharma*, et al.*, 2008). While involvement of pyruvate in the detoxification of ROS has been reported, the role of KG in alleviating the oxidative burden is beginning to be appreciated (Nakamichi*, et al.*, 2005, Brookes*, et al.*, 2006, Mailloux*, et al.*, 2007). These data clearly point to a pivotal role of histidine metabolism in the homeostasis of

KG and reveals how this aminoacid is a key component of the anti-oxidative defense strategy in *P.fluorescens*.

Concluding Remarks

This report provides further evidence on the significance of metabolism and KG in the detoxification of ROS. It adds to the growing body of literature on the role of ketoacids in anti-oxidative defense. *P.fluorescens* reprograms its metabolic networks in an effort to generate KG, a moiety that subsequently nullifies H_2O_2 with the concomitant formation of succinate and CO_2. Since histidine was utilized as the only source of nitrogen, the production of glutamate was favoured. However, this amino acid appeared to be dedicated to the production of KG, as GDH was upregulated. The inability of fluorocirate to have any inhibitory influence on KG production in the H_2O_2 - stressed cells when both citrate and histidine were present, clearly points to the pivotal role this keto acid plays in fending the oxidative environment to which *P.fluorescens* was exposed.

Since the demand for KG is critical during oxidative stress, the formation of this ketoacid is preferentially mediated by GDH in H_2O_2-challenged cells. And as its utilization via the TCA cycle is curtailed due to the down-regulation of KGDH and the complexes of the electron transport chain (ETC), the pool of KG acts as a potent weapon against H_2O_2. Hence, by reconfiguring its metabolism and channeling glutamate, a product of histidine catabolism, toward KG formation, *P.fluorescens* modulates the intracellular concentration of this ketoacid. KG is an effective scavenger of ROS and its diversion from the TCA cycle further diminishes oxidative tension as the production of

the pro-oxidant NADH is decreased (Figure 7). This anti-oxidative tactic not only helps neutralize H_2O_2 but also ensures the increased production of NADPH and diminished formation of NADH, a promoter of ROS production.

Acknowledgements:

This work was supported by Industry Canada. J.Lemire is a recipient of Alexander Graham Bell Canada doctoral fellowship

Literature Cited:

Baker PJ, Britton KL, Engel PC, Farrants GW, Lilley KS, Rice DW & Stillman TJ (1992) Subunit assembly and active site location in the structure of glutamate dehydrogenase. *Proteins* **12**: 75-86.

Beriault R, Chenier D, Singh R, Middaugh J, Mailloux R & Appanna V (2005) Detection and purification of glucose 6-phosphate dehydrogenase, malic enzyme, and NADP-dependent isocitrate dehydrogenase by blue native polyacrylamide gel electrophoresis. *Electrophoresis* **26**: 2892-2897.

Bradford MM (1976) A rapid and sensitive method for the quantitation of microgram quantities of protein utilizing the principle of protein-dye binding. *Anal Biochem* **72**: 248-254.

Brookes PS, Freeman RS & Barone MC (2006) A shortcut to mitochondrial signaling and pathology: a commentary on "Nonenzymatic formation of succinate in mitochondria under oxidative stress". *Free Radic Biol Med* **41**: 41-45.

Cabiscol E, Tamarit J & Ros J (2000) Oxidative stress in bacteria and protein damage by reactive oxygen species. *Int Microbiol* **3**: 3-8.

Cappellini MD & Fiorelli G (2008) Glucose-6-phosphate dehydrogenase deficiency. *Lancet* **371**: 64-74.

Chen Q, Vazquez EJ, Moghaddas S, Hoppel CL & Lesnefsky EJ (2003) Production of reactive oxygen species by mitochondria: central role of complex III. *J Biol Chem* **278**: 36027-36031.

Chenier D, Beriault R, Mailloux R, Baquie M, Abramia G, Lemire J & Appanna V (2008) Involvement of fumarase C and NADH oxidase in metabolic adaptation of *Pseudomonas fluorescens* cells evoked by aluminum and gallium toxicity. *Appl Environ Microbiol* **74**: 3977-3984.

DeJong RJ, Miller LM, Molina-Cruz A, Gupta L, Kumar S & Barillas-Mury C (2007) Reactive oxygen species detoxification by catalase is a major determinant of fecundity in the mosquito *Anopheles gambiae*. *Proc Natl Acad Sci U S A* **104**: 2121-2126.

Dringen R (2005) Oxidative and antioxidative potential of brain microglial cells. *Antioxid Redox Signal* **7**: 1223-1233.

Fedotcheva NI, Sokolov AP & Kondrashova MN (2006) Nonezymatic formation of succinate in mitochondria under oxidative stress. *Free Radic Biol Med* **41**: 56-64.
Finkel T & Holbrook NJ (2000) Oxidants, oxidative stress and the biology of ageing. *Nature* **408**: 239-247.
Henke B, Girzalsky W, Berteaux-Lecellier V & Erdmann R (1998) IDP3 encodes a peroxisomal NADP-dependent isocitrate dehydrogenase required for the beta-oxidation of unsaturated fatty acids. *J Biol Chem* **273**: 3702-3711.
Imlay JA (2008) Cellular defenses against superoxide and hydrogen peroxide. *Annu Rev Biochem* **77**: 755-776.
James AM, Cocheme HM, Smith RA & Murphy MP (2005) Interactions of mitochondria-targeted and untargeted ubiquinones with the mitochondrial respiratory chain and reactive oxygen species. Implications for the use of exogenous ubiquinones as therapies and experimental tools. *J Biol Chem* **280**: 21295-21312.
Li SF, Liu HX, Zhang YB, Yan YC & Li YP (2009) The protective effects of alpha-ketoacids against oxidative stress on rat spermatozoa in vitro. *Asian J Androl*.
Ludwig B, Bender E, Arnold S, Huttemann M, Lee I & Kadenbach B (2001) Cytochrome C oxidase and the regulation of oxidative phosphorylation. *Chembiochem* **2**: 392-403.
Maaty WS, Wiedenheft B, Tarlykov P*, et al.* (2009) Something old, something new, something borrowed; how the thermoacidophilic archaeon *Sulfolobus solfataricus* responds to oxidative stress. *PLoS One* **4**: e6964.
Mailloux RJ, Puiseux-Dao S & Appanna VD (2009) Alpha-ketoglutarate abrogates the nuclear localization of HIF-1alpha in aluminum-exposed hepatocytes. *Biochimie* **91**: 408-415.
Mailloux RJ, Singh R, Brewer G, Auger C, Lemire J & Appanna VD (2009) Alpha-ketoglutarate dehydrogenase and glutamate dehydrogenase work in tandem to modulate the antioxidant alpha-ketoglutarate during oxidative stress in *Pseudomonas fluorescens*. *J Bacteriol* **191**: 3804-3810.
Mailloux RJ, Beriault R, Lemire J, Singh R, Chenier DR, Hamel RD & Appanna VD (2007) The tricarboxylic acid cycle, an ancient metabolic network with a novel twist. *PLoS One* **2**: e690.
Middaugh J, Hamel R, Jean-Baptiste G, Beriault R, Chenier D & Appanna VD (2005) Aluminum triggers decreased aconitase activity via Fe-S cluster disruption and the overexpression of isocitrate dehydrogenase and isocitrate lyase: a metabolic network mediating cellular survival. *J Biol Chem* **280**: 3159-3165.
Murphy MP (2009) How mitochondria produce reactive oxygen species. *Biochem J* **417**: 1-13.
Nakamichi N, Kambe Y, Oikawa H*, et al.* (2005) Protection by exogenous pyruvate through a mechanism related to monocarboxylate transporters against cell death induced by hydrogen peroxide in cultured rat cortical neurons. *J Neurochem* **93**: 84-93.
Nasser Y, Fernandez E, Keenan CM*, et al.* (2006) Role of enteric glia in intestinal physiology: effects of the gliotoxin fluorocitrate on motor and secretory function. *Am J Physiol Gastrointest Liver Physiol* **291**: G912-927.
Prell J & Poole P (2006) Metabolic changes of rhizobia in legume nodules. *Trends Microbiol* **14**: 161-168.
Schagger H & von Jagow G (1991) Blue native electrophoresis for isolation of membrane protein complexes in enzymatically active form. *Anal Biochem* **199**: 223-231.

Sharma AB, Barlow MA, Yang SH, Simpkins JW & Mallet RT (2008) Pyruvate enhances neurological recovery following cardiopulmonary arrest and resuscitation. *Resuscitation* **76**: 108-119.
Singh R (2005) The Modulation of NADPH, NADH, and α-ketoglutarate in *P.fluorescens* exposed to oxidative stress. Masters Thesis, Laurentian University, Sudbury, Ontario.
Singh R, Mailloux RJ, Puiseux-Dao S & Appanna VD (2007) Oxidative stress evokes a metabolic adaptation that favors increased NADPH synthesis and decreased NADH production in *Pseudomonas fluorescens*. *J Bacteriol* **189**: 6665-6675.
Singh R, Lemire J, Mailloux RJ & Appanna VD (2008) A novel strategy involved in anti-oxidative defense: the conversion of NADH into NADPH by a metabolic network. *PLoS One* **3**: e2682.
Smeets K, Cuypers A, Lambrechts A, Semane B, Hoet P, Van Laere A & Vangronsveld J (2005) Induction of oxidative stress and antioxidative mechanisms in *Phaseolus vulgaris* after Cd application. *Plant Physiol Biochem* **43**: 437-444.
Starkov AA, Fiskum G, Chinopoulos C, Lorenzo BJ, Browne SE, Patel MS & Beal MF (2004) Mitochondrial alpha-ketoglutarate dehydrogenase complex generates reactive oxygen species. *J Neurosci* **24**: 7779-7788.
Thomas C, Mackey MM, Diaz AA & Cox DP (2009) Hydroxyl radical is produced via the Fenton reaction in submitochondrial particles under oxidative stress: implications for diseases associated with iron accumulation. *Redox Rep* **14**: 102-108.
Touati D (2000) Iron and oxidative stress in bacteria. *Arch Biochem Biophys* **373**: 1-6.
Valderrama R, Corpas FJ, Carreras A*, et al.* (2006) The dehydrogenase-mediated recycling of NADPH is a key antioxidant system against salt-induced oxidative stress in olive plants. *Plant Cell Environ* **29**: 1449-1459.
Zielke HR, Zielke CL, Baab PJ & Tildon JT (2007) Effect of fluorocitrate on cerebral oxidation of lactate and glucose in freely moving rats. *J Neurochem* **101**: 9-16.

Figure Captions:

Figure 1: Growth and nutrient consumption in *P.fluorescens*. *P.fluorescens* was grown in control and stressed conditions to assess cellular growth patterns. **– (closed line)** corresponds to cellular yield of control cultures. **-- (broken line)** corresponds to cellular yield of stressed culture. The consumption of citrate and histidine the primary nutrients was monitored by HPLC. ■ (gray) = histidine in control media. □ (white) = histidine in 500 μM H_2O_2 media. ■ (black) = citrate in control media. ▦ (striped) = citrate in the H_2O_2 supplemented media. n=3 ± SD. $P \leq 0.05$

Figure 2: HPLC analyses of intracellular metabolites. The CFE was isolated from **A)** control and **B)** stressed cultures. The CFE was then subjected to HPLC analysis to ascertain histidine, citrate, KG, and succinate levels. n=3 ± SD. $P \leq 0.05$

Figure 3: In-gel activity analysis of enzymes involved in α-KG homeostasis. CFE was isolated from *P.fluorescens* grown in **A)** control and **B)** H_2O_2 growth conditions. **I)** ICDH-NAD, **II)** ICDH-NADP, **III)** GDH-NAD, **IV)** GDH-NADP, **V)** KGDH, **VI)** GS and **VII)** AST. Membrane CFE were utilized for GDH-NAD, ICDH-NAD, KGDH, and GS, while soluble CFE were the source of GDH-NADP, AST, and ICDH-NADP.

Figure 4: In-gel activity analysis of enzymes involved in energy production. Membrane CFE obtained from **A)** control and **B)** H_2O_2 stressed *P.fluorescens*. **I)** SDH, **II)** Complex I, and **III)** Complex IV.

Figure 5: Regulation of enzymes involved in α-KG production. CFE was isolated from *P.fluorescens* grown in **A)** control, **B)** 100 μM H_2O_2, **C)** 500 μM H_2O_2. Control cells were recovered in 500 μM H_2O_2 for 8h **(D)**. While 500 μM H_2O_2 stressed cells were recovered in control media for 8h **(E).** Enzyme activity was determined for **I)** KGDH **II)** GDH-NAD. Expression was ascertained by immunoblotting for **III)** GDH-NAD. The 45kDa corresponds to the molecular mass of GDH homohexamer (48 – 55kDa monomer) (Baker*, et al.*, 1992)

Figure 6: KG is derived predominantly from histidine in H_2O_2 - stressed *P.fluorescens*. CFE from control, 100μM H_2O_2, and 500 μM H_2O_2 treated *P.fluorescens* was incubated with 5mM histidine, 5mM citrate, and in the absence (closed bar = ■) and presence (open bar = □) of 5mM flurocitrate for 30 min. α-KG levels were then measured using HPLC. n=3 ± SD. $P \leq 0.05$

Figure 7: Histidine as a generator of KG in *P.fluorescens* subjected to H_2O_2 insult. (ETC = electron transport chain) ↓ = decrease, ↑ = increase

Figure 1:

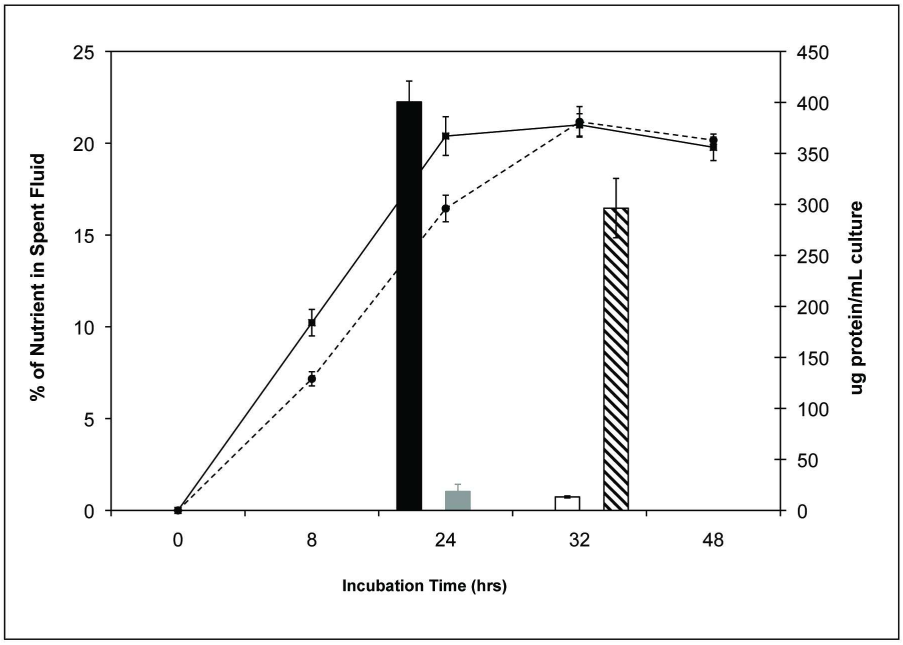

Figure 1: Growth and nutrient consumption in P.fluorescens. P.fluorescens was grown in control and stressed conditions to assess cellular growth patterns. – (closed line) corresponds to cellular yield of control cultures. -- (broken line) corresponds to cellular yield of stressed culture. The consumption of citrate and histidine the primary nutrients was monitored by HPLC. ν (gray) = histidine in control media. □ (white) = histidine in 500 μM H_2O_2 media. ν (black) = citrate in control media. ▦ (striped) = citrate in the H_2O_2 supplemented media. n=3 ± SD. $P \leq 0.05$

Figure 2:

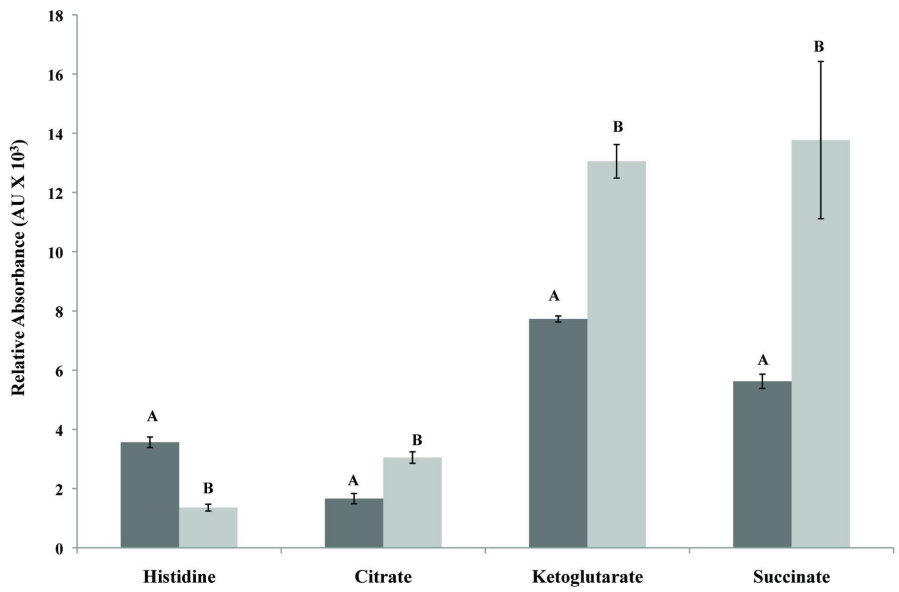

Figure 2: HPLC analyses of intracellular metabolites. The CFE was isolated from A) control and B) stressed cultures. The CFE was then subjected to HPLC analysis to ascertain histidine, citrate, KG, and succinate levels. n=3 ± SD. $P \leq 0.05$

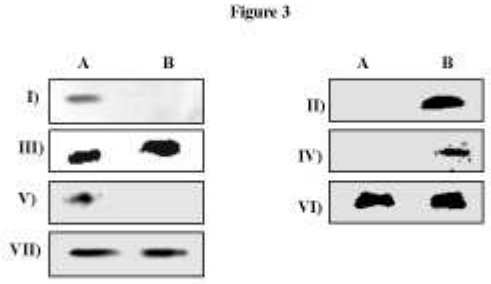

Figure 3: In-gel activity analysis of enzymes involved in α-KG homeostasis. CFE was isolated from P.fluorescens grown in A) control and B) H2O2 growth conditions. I) ICDH-NAD, II) ICDH-NADP, III) GDH-NAD, IV) GDH-NADP, V) KGDH, VI) GS and VII) AST. Membrane CFE were utilized for GDH-NAD, ICDH-NAD, KGDH, and GS, while soluble CFE were the source of GDH-NADP, AST, and ICDH-NADP.
59x31mm (200 x 200 DPI)

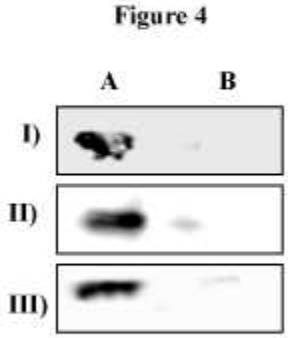

Figure 4: In-gel activity analysis of enzymes involved in energy production. Membrane CFE obtained from A) control and B) H2O2 stressed P.fluorescens. I) SDH, II) Complex I, and III) Complex IV.
50x50mm (200 x 200 DPI)

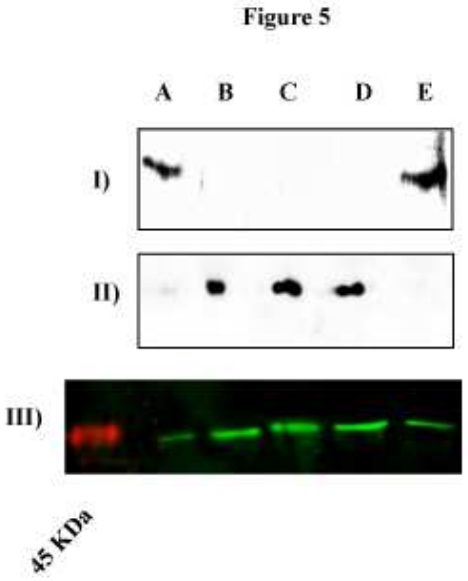

Figure 5: Regulation of enzymes involved in α-KG production. CFE was isolated from P.fluorescens grown in A) control, B) 100 µM H2O2, C) 500 µM H2O2. Control cells were recovered in 500 µM H2O2 for 8h (D). While 500 µM H2O2 stressed cells were recovered in control media for 8h (E). Enzyme activity was determined for I) KGDH II) GDH-NAD. Expression was ascertained by immunoblotting for III) GDH-NAD. The 45kDa corresponds to the molecular mass of GDH homohexamer (48 – 55kDa monomer) (Baker, et al., 1992)
59x80mm (200 x 200 DPI)

Figure 6:

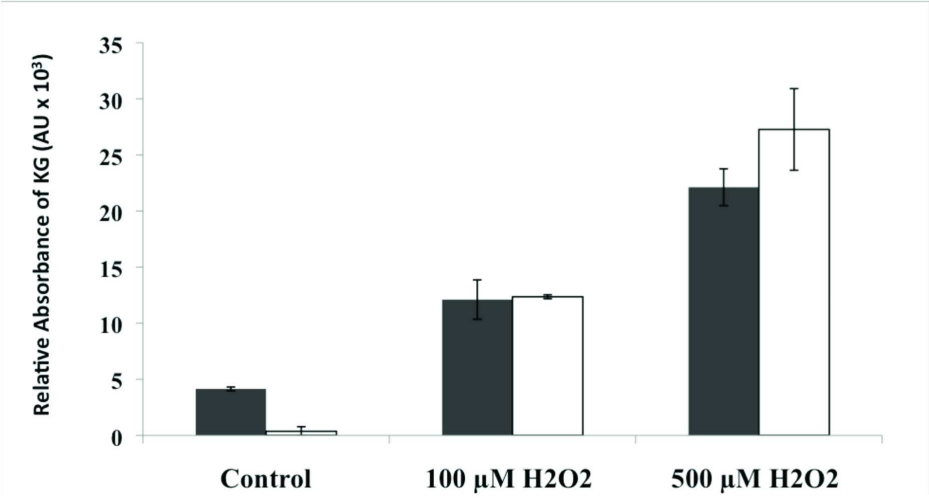

Figure 6: KG is derived predominantly from histidine in H2O2 - stressed P.fluorescens. CFE from control, 100µM H2O2, and 500 µM H2O2 treated P.fluorescens was incubated with 5mM histidine, 5mM citrate, and in the absence (closed bar = ν) and presence (open bar = □) of 5mM flurocitrate for 30 min. α-KG levels were then measured using HPLC. n=3 ± SD. P ≤ 0.05
100x64mm (508 x 508 DPI)

Figure 7:

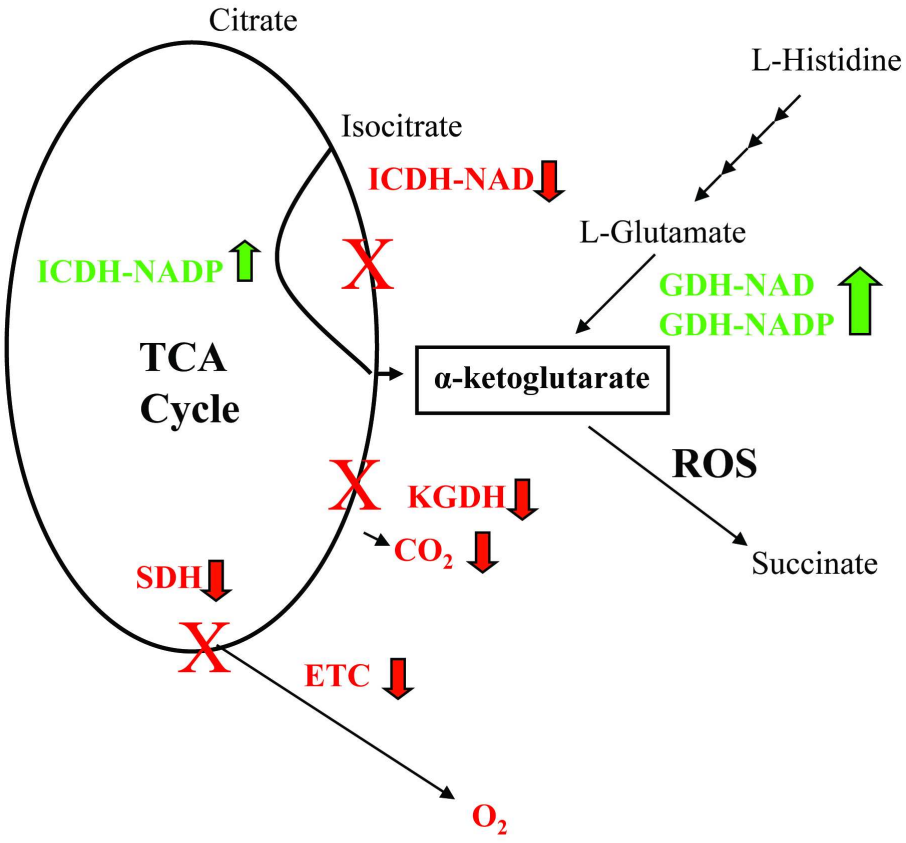

Figure 7: Histidine as a generator of KG in P.fluorescens subjected to H2O2 insult. (ETC = electron transport chain) ↓ = decrease, ↑ = increase